



HAL
open science

On the interest of a semi-empirical model for the tooth friction coefficient in gear transmissions

Romain Quiban, Nicolas Grenet de Bechillon, Thomas Touret, Pierre Navet, Yasser Diab, Jérôme Cavoret, Fabrice Ville, Christophe Changenet

► To cite this version:

Romain Quiban, Nicolas Grenet de Bechillon, Thomas Touret, Pierre Navet, Yasser Diab, et al.. On the interest of a semi-empirical model for the tooth friction coefficient in gear transmissions. Proceedings of the Institution of Mechanical Engineers, Part J: Journal of Engineering Tribology, 2021, 235 (12), pp.2654-2663. 10.1177/135065012111052179 . hal-03659960

HAL Id: hal-03659960

<https://hal.science/hal-03659960v1>

Submitted on 16 May 2023

HAL is a multi-disciplinary open access archive for the deposit and dissemination of scientific research documents, whether they are published or not. The documents may come from teaching and research institutions in France or abroad, or from public or private research centers.

L'archive ouverte pluridisciplinaire **HAL**, est destinée au dépôt et à la diffusion de documents scientifiques de niveau recherche, publiés ou non, émanant des établissements d'enseignement et de recherche français ou étrangers, des laboratoires publics ou privés.



Distributed under a Creative Commons Attribution - NonCommercial 4.0 International License

On the interest of a semi-empirical model for the tooth friction coefficient in gear transmissions

Romain Quiban¹, Nicolas Grenet De Bechillon^{1,2},
Thomas Touret² , Pierre Navet^{1,2}, Yasser Diab¹,
Jérôme Cavoret¹, Fabrice Ville¹  and Christophe Changenet²

Abstract

Accurate modelling of friction coefficient is of primary importance in efficiency, vibration and failure analyses of enclosed gear drives. After showing the influence of surface/lubricant interactions on friction, the authors used a semi-empirical model which can take all these aspects into account. Lubricant is modelled as an Eyring–Reynolds fluid and rough surfaces are described with two parameters *via* a stochastic approach. A specific two-disc machine is used to perform series of friction measurements on smooth and rough discs. Smooth discs allow to operate under full film lubrication and to measure a reference shear stress of lubricant, whereas rough discs reproduce gear tooth roughness and generate a representative value of friction on asperities. The purpose of this present paper is to describe calculations of this physical-based friction coefficient model and to present the experimental process. On the basis of new results, the impact of a surface finishing process is assessed as well as the consequence of calculating friction coefficient based on oil injection instead of local bulk temperature.

Keywords

Friction, boundary regime, mixed regime, two discs, gears

Introduction

Sliding friction at tooth contact is one of the main sources of power loss in geared transmissions as well as a potential source of vibration and noise. Its estimation is necessary for engineering purposes especially in a context where environmental concern drives the industry to more severe operating conditions. Accurate modelling of friction coefficient is therefore of primary importance in efficiency, vibration analyses and failure of mechanical transmissions.

In their monograph entitled ‘Elasto-hydrodynamic lubrication: the fundamentals of roller and gear lubrication’, Dowson & Higginson described in detail about Elasto-Hydrodynamic Lubrication (EHL) from a theoretical, experimental and applied point of view.¹ In chapter 13 of this monograph, they applied their modelling to involute spur gears. They showed that contact conditions and thus film thickness vary along the line of action and gave abacus to evaluate film thickness depending on viscosity, gear ratio and load. In chapter 10, written by J.F. Archard & A.W. Crook, the authors dealt with friction, and they emphasised the importance of thermal aspects

to accurately determine oil film thickness and friction which are intimately linked. It must be noticed this interesting sentence at the end of the chapter: ‘Now, in addition, the disk machine can be seen as an instrument for study of the rheological properties of oils in conditions of high pressure and transient stress’.

Nowadays, it is obvious that friction coefficient depends on multiple parameters (e.g. load, speed, temperature, surface roughness, solid and fluid physical properties, etc.). Its estimation is therefore complex and true prediction is still at an early stage.^{2,3} Numerical approach are possible,^{4,5} to do so most of the previous work use model based various arrangements of the Reynolds equation. Modelling can include roughness⁴ and solve the problem considering gear

¹Univ Lyon, INSA Lyon, CNRS, LaMCoS, UMR5259, Villeurbanne, France

²Univ Lyon, ECAM Lyon, LabECAM, Lyon, France

Corresponding author:

Thomas Touret, Univ Lyon, ECAM Lyon, LabECAM, Lyon 69321, France.

Email: Thomas.touret@ecam.fr

geometry and operating conditions.^{6–8} They can also be coupled with contact dynamics or include complex rheology behaviour such as shear thinning.⁹ This approach has the advantage of being very flexible and offers the possibility of investigating specific contact problematics. Yet, it can be computer intensive and difficult to set up when one aims at evaluating friction coefficient for industrial purposes such as gear optimisation.

Another approach is based on analytical formulations. In order to cope with the complexity of the contact problem, most of them are based on semi-empirical model that requires, to some extent, an empirically fitted part. Disc tribometers or two-disc machines¹⁰ are suited to reproduce tooth contacts as they can generate line or elliptical contacts with high heat flow density, similar to the ones that occur in gears. Main parameters influencing lubricated contacts such as geometry, operating conditions, material properties and environment can be modified easily in a wide range. Various empirical friction laws based on two-disc machine measurements can be found in the literature.^{11–18} One of their limitations comes from the specimen surface roughness, which is often different from the one of actual gears. In fact, most of the gear teeth are cross grounded with roughness oriented in the axial direction. A part of the above-mentioned studies used circumferentially grounded discs^{14–18} which leads to significantly different interactions between asperities. The other part^{11–13} used smooth discs which are not able to reproduce mixed lubrication. Castro and Seabra¹⁹ showed that the evaluation of friction between gear teeth, at a single contact point or along the meshing line, requires a mixed film lubrication model able to analyse the contact in full film and boundary regime and balancing between these two extreme conditions. This approach has the advantage of being simpler to solve numerically. On the other hand, it requires to generate experimental results consistent with the targeted application.

In this paper, the authors used an existing semi-empirical model of the mixed friction coefficient in non-conformal rolling–sliding contact²⁰ to highlight how an analytical approach, as well as numerical ones, can model the impact of roughness features, contact temperatures, physical and chemical interactions on the friction coefficient. This friction is considered as the sum of both fluid and asperities contribution. The model is implemented on a two-disc machine with operating conditions which covers gear applications. A series of friction coefficient measurements are performed on both smooth and rough discs. Smooth discs allow to operate under full film lubrication. In this condition, the two-disc machine is used to measure a reference shear stress of the lubricant.^{21–28} Rough discs reproduce roughness magnitude and orientation of gear teeth to estimate a representative value of friction on asperities. A discussion is given on the effect of surface finishing process on a rough surface and how it is considered in the present model.

In gear application, kinematics is such that sliding speed is important and corresponding thermal phenomena cannot

be neglected for friction prediction.^{29–31} The local rise in temperature influences both oil film thickness and friction at tooth contact. Isaac³² showed that bulk temperature has an influence on friction. In practice, gear bulk temperature is seldom known and the temperature used as a reference for tooth friction prediction is often either the one of oil jet or oil bath, depending on lubrication solution. This subject is discussed in light of new results and an adaptation of the existing friction model is presented.

Theory and calculation

Evolution of friction coefficient and associated physical phenomena are different depending on the value of reduced oil film thickness in the contact or hydrodynamic roughness parameter of Tallian³³:

$$\Lambda = \frac{h_c}{\sigma} \quad (1)$$

with Λ the reduced oil film thickness, h_c the isothermal oil film thickness at the contact centre under fully flooded conditions, σ the composite roughness defined such as $\sigma = \sqrt{Rq_1^2 + Rq_2^2}$, and Rq_1 , Rq_2 the root mean square (RMS) roughness of surface 1 and 2. Gear contacts operate mostly in mixed lubrication regimes.^{29,34,35}

Diab et al. model²⁰

In the present study, the authors use the semi-empirical model of sliding friction coefficient of non-conformal rolling–sliding contacts developed by Diab et al.²⁰ This model has the advantage of including a complete set of equations to simulate a mixed lubricated contact. This is why it was chosen as it gives acceptable results under various operating conditions. In the original model, a strong coupling was implemented between the gear dynamic model and the evaluation of the friction coefficient. The originality of this paper is to show that it is possible to decouple the dynamic solving from the analytical friction evaluation while obtaining a reliable friction coefficient. It also includes a discussion of the surface finish and how thermal aspects are included in the model based on recent studies.

All physical parameters used in the following equations are mean values over the contact area.

Normal load (F_n) is decomposed into two parts (i) one supported by surface roughness asperities referred as asperity part with subscript ‘a’ and (ii) one supported by oil film referred to as fluid part with subscript ‘f’ (equation (2)). In the same way, apparent contact area of Hertz³⁶ (A_0) is decomposed into an actual contact area (A_a) and the complementary fluid area (A_f) (equation (3)).

$$F_n = F_{n,a} + F_{n,f} \quad (2)$$

$$A_0 = A_a + A_f \quad (3)$$

Thereby, a mixed friction coefficient formula (equation (5)) is expressed in terms of shear stresses, using

equations (2)–(3) and Coulomb's law³⁷ (equation (4)).

$$\mu = \frac{F_t}{F_n} = \frac{\tau}{p} \quad (4)$$

$$\mu = \frac{1}{p} \left[\frac{A_a}{A_0} \tau_a + \left(1 - \frac{A_a}{A_0} \right) \tau_f \right] \quad (5)$$

with μ the friction coefficient, p the mean contact pressure, τ_a the shear stress from asperities and τ_f the shear stress in fluid film.

Fluid contribution

To take into account the non-Newtonian behaviour in EHL,³⁸ fluid shear stress (τ_f , equation (6)) is reformulated here in terms of a Newtonian shear stress (τ_N , equation (7))³⁹ and a reference shear stress, called Eyring stress (τ_E , equation (8)).^{40,41} This last one depends on both pressure and temperature.²⁶ Experimental constants C_0 , C_p , C_T in Houpert et al. formula^{25,42} (equation (8)) are determined using smooth discs to carry out several full film EHL traction curves at different operating., taking into account thermal effects occurring in traction tests.²⁶

Lubricant pressure in the contact (p_f , equation (10)) is derived from both load and area sharing (equations (2) and (3)). Note that smooth disc surfaces have sufficiently low roughness amplitude compared to lubricant film thickness to avoid any contact between asperities ($h_c/\sigma > 7$, $A_a/A_0 = 0$). In this case, the whole load is lifted by fluid film, inducing fluid pressure equals to Hertz mean pressure.³⁶

$$\tau_f = \tau_E \sin h^{-1} \left(\frac{\tau_N}{\tau_E} \right) \quad (6)$$

$$\tau_N = \eta_{(T_c, p_f)} \frac{v_s}{\phi_T h_c} \quad (7)$$

$$\tau_E = C_0 e^{(C_p p_f)} e^{C_T \left(\frac{1}{T_c} - \frac{1}{T_0} \right)} \quad (8)$$

$$\phi_T = \frac{1 - 13.2(p_0 / E') L_T^{0.42}}{1 + 0.213(1 + 2.23 |SRR|^{0.83}) L_T^{0.64}} \quad (9)$$

$$p_f = \frac{F_{n,f}}{A_f} = \frac{p - p_a \cdot A_a / A_0}{1 - A_a / A_0} \quad (10)$$

with *versus* the sliding speed, h_c the isothermal fully flooded central film thickness suggested by Hamrock and Dowson^{43,44} and ϕ_T the thermal reduction due to inlet backflow, revised by Gupta et al.²⁷ Oil dynamic viscosity evolution with temperature $\eta(T)$ is calculated with Vogel model⁴⁵ (equation (11)) and evolution with pressure $\eta(p)$ with Roelands model⁴⁶ (equation (13)). Following the EHL problem,⁴⁷ film thickness is calculated with lubricant properties at contact conjunction inlet temperature (T_b).^{31,48} Whereas, shear stress is calculated with lubricant properties at contact temperature (T_c)

and pressure (p_f).⁴⁹

$$\eta(T, p_{atm}) = \eta_{40} e^{\beta((1/T) - (1/T_{40}))} \quad (11)$$

$$\beta = \ln \left(\frac{\eta_{100}}{\eta_{40}} \right) / \left(\frac{1}{T_{100}} - \frac{1}{T_{40}} \right) \quad (12)$$

$$\eta(T, p) = \eta(T, p_{atm}) e^{(\ln(\eta_{40}) + 9.67) \cdot ((1+p/1.98 \times 10^8)^z - 1)} \quad (13)$$

$$z = \frac{1.98 \times 10^8 \alpha}{\ln(\eta_{40}) / (6.315 \times 10^{-5})} \quad (14)$$

with $\eta_{40,100}$ lubricant dynamic viscosity values (respectively, at 40 °C and 100 °C) at ambient pressure, $T_{40} = 313.15$ K, $T_{100} = 373.15$ K, α , β the lubricant pressure–viscosity and temperature–viscosity coefficients, respectively, and z the corresponding pressure coefficient of Roelands model.

As slip increases during the traction test, heat generation tends to increase contact temperature (T_c , equation (15)). This thermal effect is shown in Figure 1, where lubricant shear stress evolution with shear rate is correlated to contact temperature in two cases (i) lightly loaded isothermal and (ii) heavily loaded non-isothermal. Contact temperature is estimated from a reference temperature representative of discs. In the initial study,²⁰ the reference temperature is set to oil jet temperature. However, it may not be accurate as it does not account for disc thermal environment and associated heat conduction and convection. Here, the local bulk temperature is used³² and a comparison between both methods is shown in section 4. The contact temperature is then estimated adding flash temperature, ΔT_f .⁵⁰ This local temperature elevation depends on the heat produced (equation (16)), contact area and a thermal resistance (R_{th} , equation (17)) due to the striction phenomenon around the moving contact. An iterative process is necessary to compute friction coefficient as friction value depends on contact temperature and *vice*

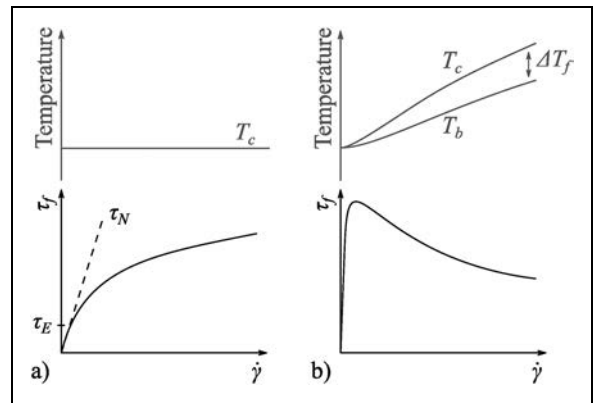


Figure 1. Effect of contact temperature on lubricant shear stress evolution with shear rate. (a) Lightly loaded (isothermal) and (b) heavily loaded (non-isothermal).

versa.²⁹

$$T_c = T_b + \Delta T_f = T_b + Q \frac{R_{th}}{A_0} \quad (15)$$

$$Q = F_n \mu v_s \quad (16)$$

$$R_{th} = 0.636 \frac{2\sqrt{2a}}{\sqrt{\pi k_1 \rho_1 c_1 v_1} + \sqrt{\pi k_2 \rho_2 c_2 v_2}} \quad (17)$$

Contribution of asperities

The second contribution of Diab et al.²⁰ model is the friction due to interaction between asperities of both surfaces. Corresponding shear stress is given by equation (18). The friction coefficient on asperities (μ_a) depends on surface and lubricant physicochemical properties and interactions. Its value is determined from a series of traction force measurements on rough discs.

$$\tau_a = p_a \mu_a \left(1 - e^{-5.4 |SRR| \sqrt{m_2/m_0}}\right) \quad (18)$$

with p_a mean pressure on asperities, SRR the slide-to-roll ratio, and m_0 , m_2 the zeroth and second spectral moment of a roughness profile. These last correspond to the square of the RMS of height and slope of a profile (known as Rq^2 and Rdq^2 in stylus measuring devices). Spectral moments can be estimated for an equivalent contact composed of two anisotropic rough surfaces with the following equations^{51–53}:

$$m_0 = Rq_1^2 + Rq_2^2 \quad (19)$$

$$m_2 = \sqrt{Rdq_{1,s}^2 Rdq_{1,t}^2} + \sqrt{Rdq_{2,s}^2 Rdq_{2,t}^2} \quad (20)$$

indices 1 and 2 refer to disc surfaces, and indices ‘s’ for sliding direction and ‘t’ for transverse direction. Roughness parameters are obtained by the following standards.^{54–56}

To describe pressure on asperities summits, different approaches dealing with statistical formulations were proposed.^{57–60} As load supported by asperities increases, the real contact area will accordingly increase because of asperity elastic deformations. A consequence of the real contact area contact being proportional to the load is that the real contact pressure is nearly constant (equation (21)).

$$p_a = 0.1 E' \sqrt{\frac{m_2}{\pi}} \quad (21)$$

with E' the reduced elastic modulus.⁴³

The real contact area of rough elastic bodies is given by⁶²

$$\frac{A_a}{A_0} = \frac{1}{2} \cdot \frac{1}{2} \left(1 - \operatorname{erf}\left(\frac{\phi_T h_c}{\sqrt{2} m_0}\right)\right) \quad (22)$$

Table 1. Lubricant data.

Lubricant type		MIL-PRF-23699
Cinematic viscosity	ν_{40-100}	24.2; 4.97 cSt
Density	ρ_{15}	975 kg/m ³
Pressure–viscosity coefficient	α	16 GPa ⁻¹
Temperature–viscosity coefficient	β	3169 K

Test rig, specimens and methods

Test rig and specimens

As it was already underlined in the previous section, the above-mentioned model requires some experiments to determine several coefficients. The two-disc machine used in this study is presented elsewhere.^{10,61} Experiments were carried out with typical aeronautical lubricant (Table 1) and steel discs (Table 2). Some of the discs were smooth ($Ra = 0.02 \mu\text{m}$) while roughness of the others was similar to that of gears, i.e. $Ra \approx 0.3 \mu\text{m}$, with a transverse grinding direction (Figure 2).

Methods

A series of traction tests are conducted for both smooth and rough disc pairs. First, smooth disc pair measurements allow to determine the values of C_0 , C_p and C_T coefficients from Eyring stress formula (equation (8)). Indeed, smooth disc roughness amplitude is sufficiently low in front of lubricant film thickness to ensure that traction is mainly due to fluid shearing. Then, rough disc traction curves allow to determine a value of friction on asperities (μ_a) of the surface/lubricant. The values of these parameters are computed using an algorithm that minimises the difference between calculations and experimental results.

Measurements are performed for (i) three rolling speeds, (ii) three contact pressures and (iii) three lubricant injection temperatures. This forms a total of 2×27 traction tests allowing accurate estimations of experimental

Table 2. Discs data.

Grinding direction Material	Smooth		Rough	
	Sliding (circumferential)		Transverse (axial)	
	Nitrided steel			
E' (GPa)	231			
L (mm)	10			
R_x (mm)	35			
R_y (mm)	∞	200	∞	200
Ra (μm)	0.02	0.02	0.42	0.29
Rq (μm)	0.03	0.03	0.52	0.36
Rdq_s (rad)	0.027	0.029	0.089	0.070
Rdq_t (rad)	0.033	0.029	0.026	0.025

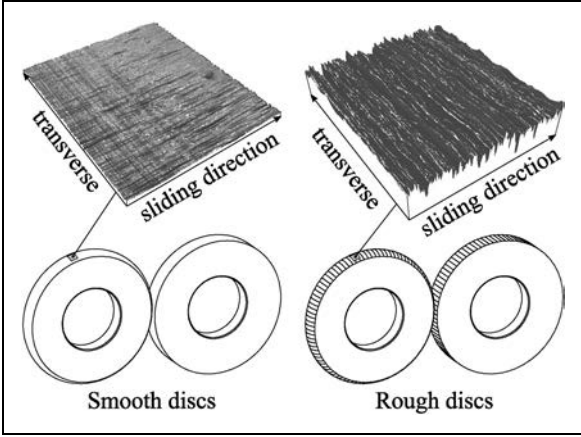


Figure 2. Specimens surface topographies.

Table 3. Operating condition during the test campaign.

Lubricant temperature	T_{inj}	40; 80; 100°C
Maximum pressure	p_o	1.2; 1.6; 1.9 GPa
Average speed	v_e	10; 20; 30 m/s
Slide-to-roll ratio	SRR	-20% to +20%

coefficients, while operating conditions are chosen to encompass gear operating conditions (Table 3). Disc bulk temperatures, for friction estimation, are obtained via a dedicated thermal model of the two-disc machine.³²

Results and discussion

Global overview of lubrication regimes encountered during the test campaign is shown in Figure 3. The measured friction coefficient value at $SRR = +20\%$ is displayed for each traction test. Smooth discs operate under full film lubrication where friction is only due to fluid shearing. Reduced film thickness ($\Lambda = h_c/\sigma$) values vary from 7.36 to 44.00. Whereas, rough discs operate under mixed lubrication with reduced film thickness values from 0.41 to 2.48. The corresponding friction coefficient value varies from 0.010 to 0.035, depending on lubricant injection temperature, transmitted load, average speed and surface roughness.

Figure 4 shows a number of experimental traction curves obtained from the two-disc machine³² as well as results given by equations (5) to (22), using values from Table 4. Influence of oil injection temperature, normal load and average speed is highlighted. It appears that there is a good agreement between experiments and calculations.

Effect of a surface finishing process

Another pair of rough discs were used, with the same geometrical and material properties as that of the previous ones, but with a surface finishing process. The process significantly reduces roughness slopes as it can be seen in the profiles measured in the sliding direction of the standard rough

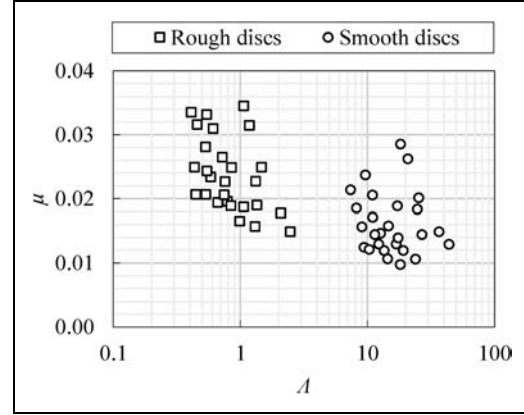


Figure 3. Measured friction coefficient at $SRR = +20\%$ for each traction curves (table 3).

disc (Figure 5(a)) and the one with finishing process (Figure 5(b)). The process was sufficiently mild so that roughness amplitudes and principal direction remain close to the one of the standard rough surfaces ($Ra_{rough} \approx 0.35 \mu\text{m}$, $Ra_{finish} \approx 0.30 \mu\text{m}$). Roughness parameters values of the finished disc pair are shown in Table 5. The main difference with the standard rough discs (Table 2) comes from the average roughness slope which is greatly reduced on the discs with a finishing process, whereas amplitude parameters values remain close.

Traction force was measured for the 27 operating conditions presented in Table 3. The friction coefficient appears to be reduced with the finished discs, especially for low film thickness conditions. Figure 6 shows measured and predicted mixed lubricated traction curves of standard and finished rough discs at oil injection temperature of (a) 40°C and (b) 100°C. At high oil temperature, the film thickness separating the two surfaces of the lubricated contact is reduced and thus reveals the friction contribution of asperities.

In the case of the finished disc, the measured friction coefficient is reduced by 20% compared to the standard rough discs, as shown in Figure 6(b). The present model accounts for the surface finishing process. The reduction of roughness slopes induces a lower pressure on asperities (equation (21)) and thus a lower contribution of asperities for the same reduced film thickness. In fact, more of the load is carried by the fluid. However, with this type of surface finish, there is a tendency to change the tribochemical properties of the surface. Thus the parameter that models the contact between surface asperities (μ_a) was also impacted. The best fit for this parameter is equal to 0.10 for the finished discs, compared to 0.11 for the standard ones. Therefore if this law is applied to gears, the process used to manufacture rough discs should be similar to the actual gear of the final application.

Effect of oil reference temperature for computation

Figure 7 shows a traction test measurement and associated numerical prediction using either oil jet or disc bulk temperature as a reference for friction calculation. It can be

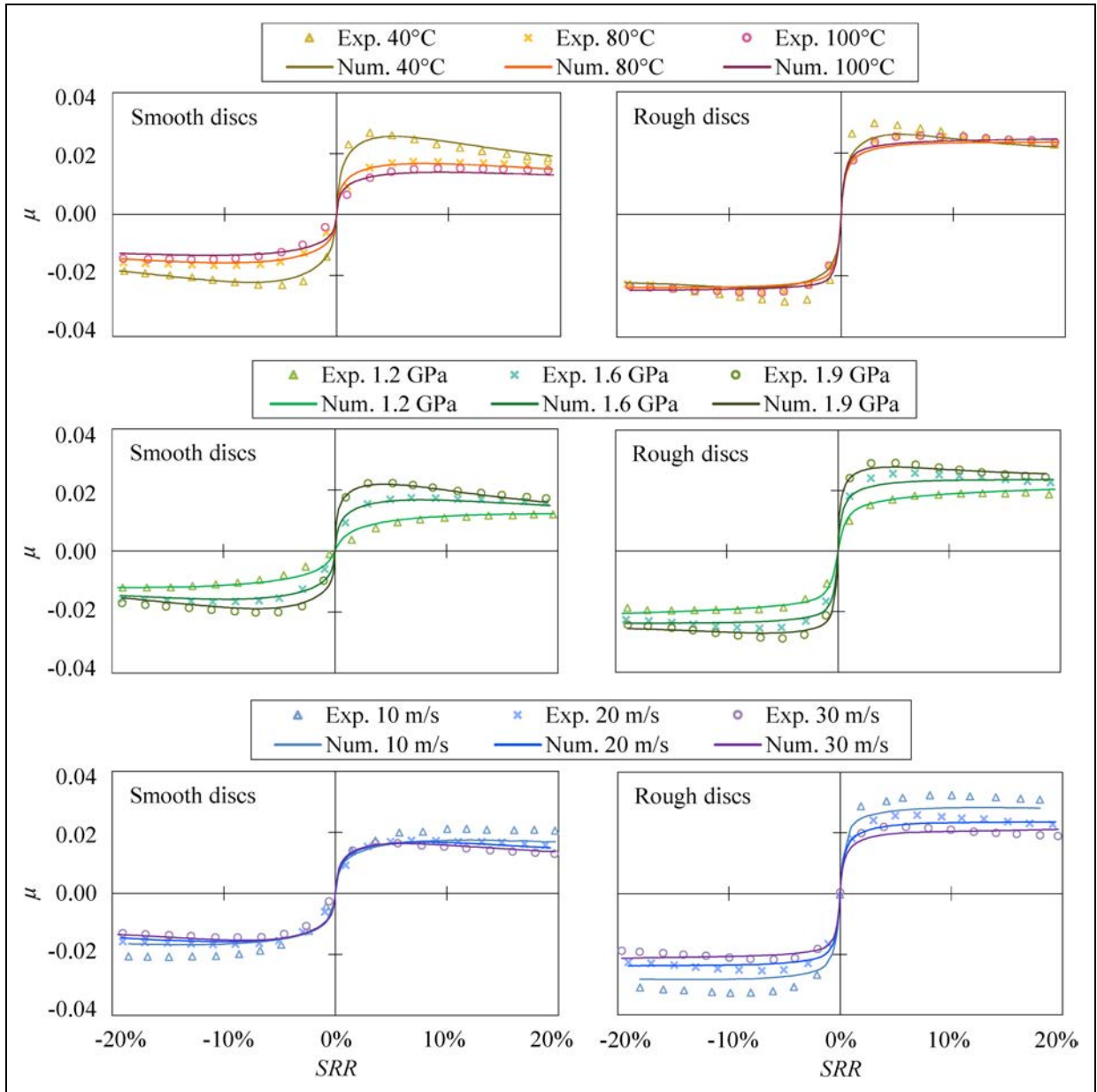


Figure 4. Experimental and numerical traction curves were obtained for smooth and rough discs. Influence of oil jet temperature, normal load and average speed. Reference condition: $T_{inj}=80^{\circ}\text{C}$, $p_0=1.6\text{ GPa}$, $v_e=20\text{ m/s}$.

Table 4. Experimental coefficients from equations (8) and (18) for nitrided steel material MIL-PRF-23699 lubricant.

C_0 (MPa)	C_p (GPa^{-1})	C_T (K)	μ_a (-)	Mean error
1.00	1.60	1500	0.11	12.7%

noticed that measurements are not exactly symmetrical for positive and negative sliding. This is due to disc warming as heat generated by friction dissipates through it. Friction values for negative sliding are slightly reduced as those measurements are operated on hotter discs. Traction curve prediction using oil injection temperature is strictly symmetrical due to constant oil jet temperature during the traction test Results remain close to experimental data as long as disc temperatures are close to the oil one,

otherwise, a significant shift is seen, typically of 30% error for temperature difference superior to 5°C in this case. Traction curve prediction using disc bulk temperature is close to measurements, with a maximum error of 10%. This shows that using oil supply temperature to estimate friction coefficient can lead to significant errors depending on disc bulk and oil supply temperature difference.

Influence of surface and lubricant on friction coefficient

As it has been pointed out in previous sections, surface finishing and temperatures (oil properties modification) have an impact on the friction coefficient. To confirm these trends, numerous friction coefficients were measured with different

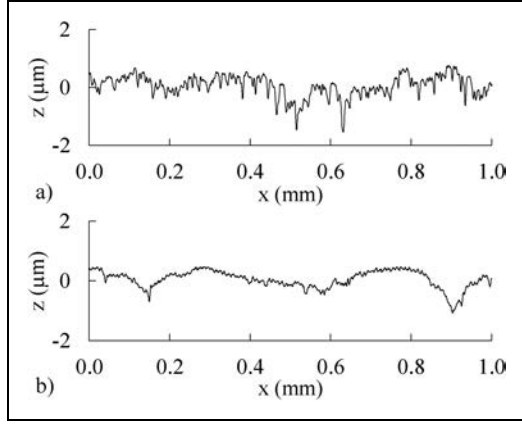


Figure 5. Measured roughness profiles of (a) rough disc surface, $R_q=0.52$, $R_{dq}=0.089$ and (b) rough disc surface with a finishing process, $R_q=0.40$, $R_{dq}=0.042$. Only a portion of the measured length is shown here for visual purpose.

Table 5. Additional discs data.

	Rough discs with surface finish	
R_x (mm)	35	
R_y (mm)	∞	200
R_a (μm)	0.32	0.26
R_q (μm)	0.40	0.33
R_{dq_s} (rad)	0.042	0.053
R_{dq_t} (rad)	0.022	0.025

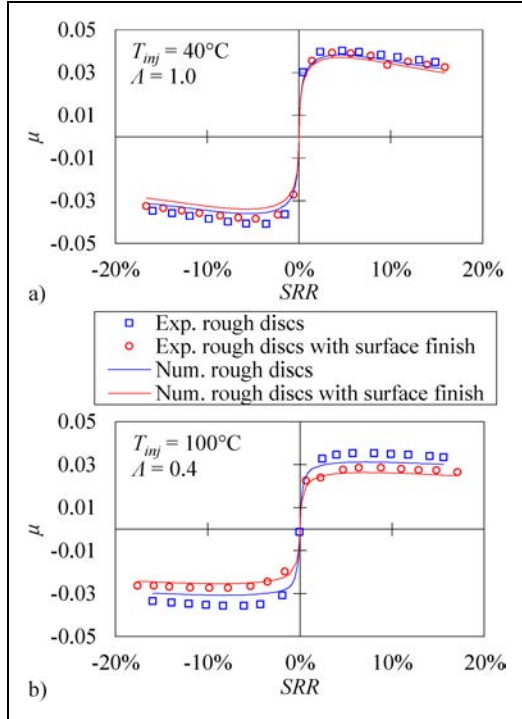


Figure 6. Effect of a surface finishing process on traction curve at $v_e = 10$ m/s and $p_0 = 1.9$ GPa. (a) $T_{inj} = 40^\circ\text{C}$ ($A = 1.0$), (b) $T_{inj} = 100^\circ\text{C}$ ($A = 0.4$).

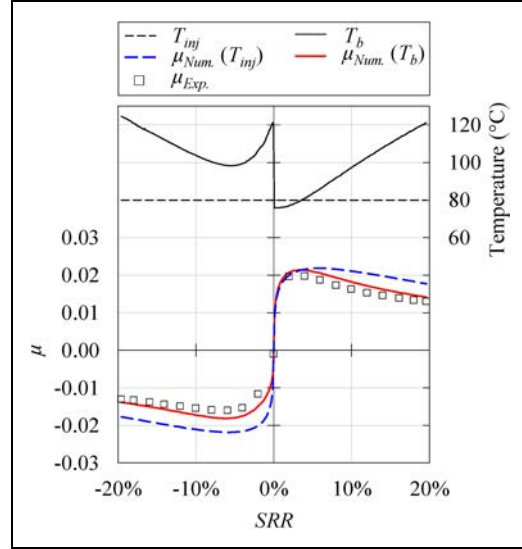


Figure 7. Traction test prediction using either oil injection or disc bulk temperature, $t_{inj} = 80^\circ\text{C}$, $p_0 = 1.9$ GPa, $v_e = 30$ m/s.

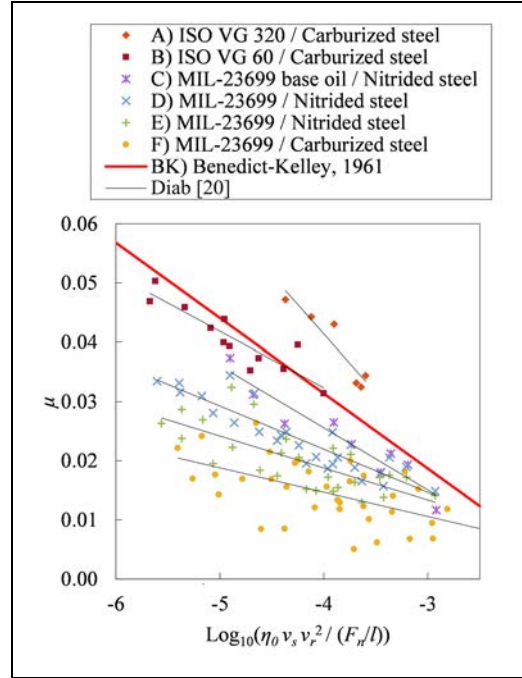


Figure 8. Two-disc friction coefficient measurements are displayed in Benedict-kelley chart.¹⁴

discs and oils to analyse if these coefficients depend on the surface and the lubricant. Friction coefficient values were obtained from direct traction measurements on a two-disc test rig (see paragraph 3). The range of experimental conditions covered is: $\eta_0 = [0.046-0.18]$ Pa.s ([5–200] cSt); $v_s = [1-6]$ m/s, $v_e = [6-30]$ m/s and $F_n/l = [150-1100]$ N/mm ($p_0 = [0.7-1.9]$ GPa).

Experimental values were compared to Diab and Benedict and Kelley laws, the latter being traditionally used in industry¹⁴ (equation (23)).

$$\mu_{BK} = a_1 \text{Log}_{10} \left(\frac{b_1 (F_n / l)}{\eta_0 v_s v_r^2} \right) \quad (23)$$

Table 6. Impact of the lubricant and material pair on the calibration of diab coefficients.

Lubricant	Disc material	R_a (μm)	C_0 (MPa)	C_p (GPa^{-1})	C_T (K)	μ_a (-)	Mean error
A ISO VG 320 mineral oil	Carburised steel	≈ 0.80	1.84	1.12	235	0.17	20.8%
B ISO VG 60 mineral oil	Carburised steel	≈ 0.80	3.26	3.24	294	0.11	13.9%
C MIL-PRF-23699 synthetic base oil	Nitrided steel	≈ 0.35	0.52	2.03	1505	0.11	17.7%
D MIL-PRF-23699 synthetic oil	Nitrided steel	≈ 0.35	1.00	1.60	1500	0.11	12.7%
E MIL-PRF-23699 synthetic oil	Nitrided steel + finish proc.	≈ 0.30	1.00	1.60	1500	0.10	13.1%
F MIL-PRF-23699 synthetic oil	Carburised steel	≈ 0.10	0.78	1.47	472	0.09	17.0%

where F_n is normal load, l total contact length, η_0 oil dynamic viscosity at contact inlet, *versus* sliding speed, v_r sum rolling speed ($=2v_e$) and a_1 , b_1 best-fit coefficients. Benedict and Kelley found $a_1=0.0127$ and $b_1=0.0297$ S.I.

As shown in Figure 8, friction coefficient values do not lie on Benedict and Kelley master curve. This means that using only oil viscosity (equation (23)) to describe the influence of the surface and the lubricant is not sufficient. The influence of roughness amplitude is noticeable as higher friction coefficients were measured during the test campaign with rougher discs (A and B in, $R_a \approx 0.8 \mu\text{m}$), whereas lower friction coefficients were measured during the test campaign with smoother discs (F, $R_a \approx 0.1 \mu\text{m}$). Finally, test campaigns C and D with the same discs and the same type of lubricant but with or without an additive package suggest that surface/lubricant interactions have a significant influence on friction. Therefore, the use of a model able to take into account surface, lubricant and surface/lubricant interactions are necessary. This is underlined by the computed values of C_0 , C_p , C_T , μ_a coefficients (Table 6). The black solid lines shown in Figure 8 represent the master curves obtained with the coefficient from Table 6.

This emphasises the importance of experimental coefficients to accurately qualify the lubricant-material interaction in a mixed lubricated contact.

Conclusion

Analysis of numerous traction measurements on two-disc machines with different discs and lubricants showed the influence of surface, lubricant and surface/lubricant interactions on friction. In addition to usual roughness amplitude parameters (e.g. R_a , R_q , R_z , etc.) to describe a surface, it was shown that roughness slopes (Rdq) can have a significant influence on friction. Likewise, it was shown that lubricant cannot be fully described by its viscosity value. Instead, it may be more accurate to also use surface/lubricant-related parameters.

The mixed friction model of Diab et al.²⁰ was used to predict two-disc machine traction curves. This model is suited to predict gear friction loss as it is developed to reproduce rough disc behaviour which is representative of gear tooth roughness. Although the model is based on simplifying assumptions, in particular the use of constant parameter over the contact, the results are close to

those measured. The present model shows average errors ranging from 12.7% to 20.8% regarding experimental data on a broad range of oils, materials and operating conditions.

The temperature to be used for the prediction of friction coefficient was discussed. It appears that using oil temperature can lead to error in friction prediction if this temperature is significantly different from the disc bulk ones.


Declaration of Conflicting Interests


The author(s) declared no potential conflicts of interest with respect to the research, authorship and/or publication of this article.

Funding

The author(s) received no financial support for the research, authorship and/or publication of this article.

ORCID iDs

Thomas Touret  <https://orcid.org/0000-0002-6165-3705>

Fabrice Ville  <https://orcid.org/0000-0002-9743-8820>

References

- Dowson D and Higginson GR. *Elasto-Hydrodynamic lubrication: the fundamentals of roller and gear lubrication*. United Kingdom: Pergamon Press, 1966.
- Björling M, Habchi W, Bair S, et al. Towards the true prediction of EHL friction. *Tribol. Int.* 2013; 66: 19–26.
- Zhu D and Hu YZ. A computer program package for the prediction of EHL and mixed lubrication characteristics, friction, subsurface stresses and flash temperatures based on measured 3-d surface roughness. *Tribol. Trans.* 2001; 44: 383–390.
- Pei J, Han X, Tao Y, et al. Mixed elastohydrodynamic lubrication analysis of line contact with Non-Gaussian surface roughness. *Tribol. Int.* 2020; 151: 106449.
- Zhang X, Li Z and Wang J. Friction prediction of rolling-sliding contact in mixed EHL. *Meas. J. Int. Meas. Confed.* 2017; 100: 262–269.
- Wu S and Cheng HS. A friction model of partial-Ehl contacts and Its application to power loss in spur gears. *Tribol. Trans.* 1991; 34: 398–407.
- Chimanpure AS, Kahraman A and Talbot D. A transient mixed elastohydrodynamic lubrication model for helical gear contacts. *J. Tribol.* 2021; 143: 1–15.
- Li S and Kahraman A. A transient mixed elastohydrodynamic lubrication model for spur gear pairs. *J. Tribol.* 2010; 132: 1–9.

9. Akbarzadeh S and Khonsari MM. Performance of spur gears considering surface roughness and shear thinning lubricant. *J. Tribol.* 2008; 130: 1–8.
10. Ville F, Nélias D, Tournalias G, et al. On the Two-disc machine: a polyvalent and powerful tool to study fundamental and industrial problems related to elastohydrodynamic lubrication. *Tribol. Ser.* 2001; 39: 393–402.
11. Kuzmin NF. Coefficient of friction in heavily loaded contact. *Vestn. Mashinostroeniya* 1954; 34: 18–26.
12. Misharin YA. Influence of the Friction Condition on the Magnitude of the Friction Coefficient in the Case of Rollers with Sliding. In: Proceedings of the International Conference on Gearing, 1958, pp.159–164. London, UK: Institution of Mechanical Engineers, London.
13. Höhn BR, Michaelis K and Doleschel A. Frictional behaviour of synthetic gear lubricants. *Tribol. Ser.* 2001; 39: 759–768.
14. Benedict GH and Kelley BW. Instantaneous coefficients of gear tooth friction. *ASLE Trans.* 1961; 4: 59–70.
15. O’Donoghue JP and Cameron A. Friction and temperature in rolling sliding contacts. *ASLE Trans.* 1966; 9: 186–194.
16. Kelley BW and Lemanski AJ. Lubrication of involute gearing. *Proc. Inst Mech. Eng.* 1967; 182: 173–184.
17. Drozdov YN and Gavrikov YA. Friction and scoring under the conditions of simultaneous rolling and sliding of bodies. *Wear* 1968; 11: 291–302.
18. Matsumoto S and Morikawa K. The New Estimation Formula of Coefficient of Friction in Rolling-Sliding Contact Surface under Mixed Lubrication Condition for the Power Loss Reduction of Power Transmission Gears. In: International Gear Conference, 2014, pp.1078–1088.
19. Castro J and Seabra J. Coefficient of friction in mixed film lubrication: gears versus twin-discs. *Proc. Inst Mech. Eng. Part J J. Eng. Tribol.* 2007; 221: 399–411.
20. Diab Y, Ville F and Vexex P. Prediction of power losses Due to tooth friction in gears. *Tribol. Trans.* 2006; 49: 260–270.
21. Smith FW. Lubricant behavior in concentrated contact—some rheological problems. *ASLE Trans.* 1960; 3: 18–25.
22. Johnson KL and Roberts AD. Observations of viscoelastic behaviour of an elastohydrodynamic lubricant film. *Proc. R. Soc. A Math. Phys. Eng. Sci.* 1974; 337: 217–242.
23. Johnson KL and Tevaarwerk JL. Shear behaviour of elastohydrodynamic Oil films. *Proc. R. Soc. A.* 1977; 356: 215–236. <https://doi.org/10.1098/rspa.1977.0129>
24. Hirst W and Moore AJ. Elastohydrodynamic lubrication at high pressures. *Proc. R. Soc. A Math. Phys. Eng. Sci.* 1978; 360: 403–425.
25. Houpert L, Flamand L and Berthe D. Rheological and thermal effects in lubricated E.H.D. Contacts. *ASME J. Lubr. Technol.* 1981; 103: 526–532.
26. Evans CR and Johnson K,L. The rheological properties of elastohydrodynamic lubricants. *Proc. Inst Mech. Eng. Part C J. Mech. Eng. Sci.* 1986; 200: 303–3012.
27. Gupta PK, Cheng HS, Zhu D, et al. Viscoelastic effects in MIL-L-7808-type lubricant, part I: analytical formulation. *Tribol. Trans.* 2008; 35: 269–274.
28. Sottomayor A, Campos A, Seabra J, et al. Experimental evaluation and numerical simulation of MIL-L-23699 traction curves: in memorium of georges tournalias. *Tribol. Ser.* 2004; 43: 795–806.
29. Olver AV. Gear lubrication—a review. *Proc. Inst Mech. Eng. Part J J. Eng. Tribol.* 2002; 216: 255–267.
30. Changenet C, Oviedo-Marlot X and Vexex P. Power loss predictions in geared transmissions using thermal networks-applications to a Six-speed manual gearbox. *J. Mech. Des.* 2006; 128: 618.
31. Liu HC, Zhang BB, Bader N, et al. Crucial role of solid body temperature on elastohydrodynamic film thickness and traction. *Tribol. Int.* 2019; 131: 386–397.
32. Isaac G, Changenet C, Ville F, et al. Thermal analysis of twin-disc machine for traction tests and scuffing experiments. *Proc. Inst Mech. Eng. Part J J. Eng. Tribol.* 2018; 232: 1548–1560.
33. Tallian TE. The theory of partial elastohydrodynamic contacts. *Wear* 1972; 21: 49–101.
34. Martin KF. A review of friction predictions in gear teeth. *Wear* 1978; 49: 201–238.
35. Hamrock J. *Fundamentals of fluid film lubrication*. 1st Ed. US: McGraw-Hill, 1994.
36. Hertz H. Über Die berührung fester elastischer körper. *J. für Reine und Angew. Math.* 1881; 92: 156–171.
37. Coulomb CA. *Théorie Des machines simples*. Paris: Bachelier, 1821, p.368.
38. Hirst W and Moore AJ. Non-Newtonian behaviour in elastohydrodynamic lubrication. *Proc. R. Soc. A Math. Phys. Eng. Sci.* 1974; 337: 101–121.
39. Newton I. *Philosophiae naturales principia mathematica*. 3rd ed. London: Cambridge University Press, 1726, p.572.
40. Eyring H. Viscosity, plasticity, and diffusion as examples of absolute reaction rates. *J. Chem. Phys.* 1936; 4: 283–291.
41. Moore AJ. The behaviour of lubricants in elastohydrodynamic contacts. *Proc. Inst Mech. Eng. Part J J. Eng. Tribol.* 1997; 211: 91–106.
42. Forster NH, Schrand JB and Gupta PK. Viscoelastic effects in MIL-L-7808-type lubricant, part II: experimental data correlations. *Tribol. Trans.* 1992; 35: 275–280.
43. Hamrock BJ and Dowson D. Isothermal elastohydrodynamic lubrication of point contacts part III — fully flooded results. *J. of Lubrication Tech.* 1977; 99 (2): 264–275.
44. Brewe DE and Hamrock BJ. Simplified solution for elliptical-contact deformation between Two elastic solids. *ASME J. Lubr. Technol.* 1977; 99: 485–487.
45. Vogel DH. Das temperaturabhaengigkeitsgesetz Der viskosität von fluessigkeiten. *Phys. Zeitschrift* 1921; 22: 645.
46. Roelands CJA, Vlugter JC and Waterman HI. The viscosity-temperature-pressure relationship of lubricating oils and Its correlation with chemical constitution. *ASME J. Basic Eng.* 1963; 11: 601–610.
47. Dowson D, Higginson GR and Whitaker AV. Elasto-Hydrodynamic lubrication: a survey of isothermal solutions. *J. Mech. Eng. Sci.* 1962; 4: 121–126.
48. Greenwood JA. Elastohydrodynamic lubrication. *Lubricants* 2020; 8. <https://doi.org/10.3390/lubricants8050051>
49. Olver AV and Spikes HA. Prediction of traction in elastohydrodynamic lubrication. *Proc. Inst Mech. Eng. Part J J. Eng. Tribol.* 2001; 215: 321–332.
50. Blok H. The flash temperature concept. *Wear* 1963; 6: 483–494.
51. Sayles R, and Thomas S and R T. Thermal conductance of a rough elastic contact. *Appl. Energy* 1976; 2: 249–267.
52. Francis HA. Application of spherical indentation mechanics to reversible and irreversible contact between rough surfaces. *Wear* 1977; 45: 221–269.
53. Manners W and Greenwood JA. Some observations on Persson’s Diffusion theory of elastic contact. *Wear* 2006; 261: 600–610.
54. *ISO 4287 - Geometrical Product Specification (GPS) – Surface Texture: Profile Method – Terms, Definitions and*

Surface Texture Parameters, 1997. <https://www.iso.org/standard/10132.html>

55. ISO 4288 - Geometrical Product Specification (GPS) – Surface Texture: Profile Method – Rules and Procedures for the Assessment of Surface Texture, 1998. <https://www.iso.org/standard/2096.html>
56. ISO 16610-21 - Geometrical Product Specification (GPS) – Filtration – Part 21: Linear Profile Filters: Gaussian Filters, 2012. <https://www.iso.org/standard/50176.html>
57. Greenwood JA and Williamson JBP. Contact of nominally flat surfaces. *Proc. R. Soc. Lond. A. Math. Phys. Sci.* 1967; 295: 300–319.
58. Longuet-Higgins MS. The statistical analysis of a random, moving surface. *Philos. Trans. R. Soc. London. Ser. A, Math. Phys. Sci.* 1957; 249: 321–387.
59. Bush AW, Gibson RD and Thomas TR. The elastic contact of a rough surface. *Wear* 1975; 35: 87–111.
60. Nayak PR. Random process model of rough surfaces. *ASME J. Lubr. Technol.* 1971; 93: 398–407.
61. Gupta PK, Flamand L, Berthe D, et al. On the traction behavior of several lubricants. *ASME J. Lubr. Technol.* 1981; 103: 55–64.
62. Mikic BB. Thermal contact conductance; theoretical considerations. *Int J Heat Mass Tran.* 1974; 17: 205–214. [https://doi.org/10.1016/0017-9310\(74\)90082-9](https://doi.org/10.1016/0017-9310(74)90082-9)

Appendix

Notation

A_0	Apparent contact area (Hertz), m^2
A_a	Actual contact area, m^2
A_f	Fluid area, m^2
a	Semi-minor width of Hertzian contact, m
b	Semi-major width of Hertzian contact, m
c	Specific heat capacity, J/(kg.K)
C_0	Eyring shear stress at reference temperature and pressure, Pa
C_p	Eyring shear stress parameter for pressure, 1/Pa
C_T	Eyring shear stress parameter for temperature, K
E_i	Young modulus of body i, Pa
E'	Reduced elastic modulus, Pa
F_n	Normal load,
$F_{n,a}$	Normal load supported by asperities, N
$F_{n,f}$	Normal load supported by fluid, N
F_t	Traction force, N
h	Mean plane separation ($= \varphi_T h_c$), m
h_c	Fully flooded isothermal central film thickness, m
k	Thermal conductivity, W/(m.K)
l	Total contact length in BK law, ($= 2b$ for disc application), m
L	Disc width, m
L_T	Thermal loading parameter ($= \frac{\beta n_0 v_e^2}{T^2 k}$)
m_0	Zeroth spectral moment of roughness ($= \sigma^2$), m^2
m_2	Second spectral moment of roughness, rad^2
p	Mean contact pressure ($= F_n / A_0$), Pa
p_0	Maximum Hertz pressure, Pa
p_{atm}	Atmospheric pressure, Pa
p_a	Pressure supported by asperities, Pa
p_f	Pressure supported by fluid, Pa

Q	Heat produced in the contact (equation (16)), W
Ra_i	Arithmetic average roughness of surface i, m
Rq_i	RMS. roughness of surface i, m
Rdq_i	RMS roughness slope of surface i in sliding or transverse direction, rad
$R_{x,i}$	Rolling radius of surface i, m
$R_{y,i}$	Crown radius of surface i, m
R_{eq}	Equivalent radius of curvature ($= (1/R_x + 1/R_y)^{-1}$), m
R_{th}	Thermal resistance of striction (equation (17)), m^2K/W
S_{crit}	Stick–slip coefficient
SRR	Slide-to-roll Ratio ($= v_s / v_e$)
T	Temperature, K
T_b	Disc bulk temperature, K
T_c	Contact temperature (equation (15)), K
v_i	Rolling speed of surface i, m/s
v_e	Average speed ($= (v_1 + v_2) / 2$), m/s
v_r	Sum rolling speed ($= v_1 + v_2$), m/s
v_s	Sliding speed ($= v_1 - v_2$), m/s

Greek letters

α	Pressure–viscosity coefficient, 1/Pa
β	Temperature–viscosity coefficient, K
Δx	Sample spacing of a roughness profile, m
$\dot{\gamma}$	Fluid shear rate, 1/s
ΔT_f	Flash temperature elevation in the contact, K
η	Absolute oil dynamic viscosity, Pa.s
η_0	Absolute oil dynamic viscosity at contact inlet, Pa.s
λ_c	High-pass filter cut-off, m
Λ	Reduced film thickness (equation (1))
μ	Friction coefficient
μ_a	Friction coefficient on asperities
ν	Absolute oil kinematic viscosity, m^2/s
ν_i	Poisson’s ratio of massif i
ρ	Density, kg/m^3
φ_T	Thermal reduction factor, Gupta et al. ²⁷
σ	Composite RMS roughness ($= \sqrt{Rq_1^2 + Rq_2^2}$)
τ_a	Shear stress due to asperities friction, Pa
τ_f	Shear stress due to fluid friction, Pa
τ_E	Eyring reference shear stress of non-Newtonian fluid, Pa
τ_N	Newtonian shear stress, Pa

Indices

1	Disc 1
2	Disc 2
n	Normal direction
s	Sliding direction
t	Transverse direction

Abbreviations

BGT	Bush, Gibson and Thomas microcontact model ⁵⁹
BK	Benedict and Kelley friction law ¹⁴
EHL	Elasto-Hydrodynamic Lubrication